Chemistry & Biology
Article

Combination of Reverse and Chemical Genetic Screens Reveals Angiogenesis Inhibitors and Targets

Mattias Kalén,[1,2,7] Elisabet Wallgard,[1,2,7] Noomi Asker,[1,8] Aidas Nasevicius,[3,9] Elisabet Athley,[1,10] Erik Billgren,[1,11] Jon D. Larson,[3,12] Shannon A. Wadman,[3,13] Elizabeth Norseng,[1,14] Karl J. Clark,[3,15] Liqun He,[2] Linda Karlsson-Lindahl,[1,8] Ann-Katrin Häger,[1,16] Holger Weber,[4,17] Hellmut Augustin,[4,18] Tore Samuelsson,[5] Chelsy K. Kemmet,[6] Carly M. Utesch,[6] Jeffrey J. Essner,[3,6] Perry B. Hackett,[3,12] and Mats Hellström[1,2,*]

[1]AngioGenetics Sweden AB, Scheeles väg 2, SE 171 77 Stockholm, Sweden
[2]Karolinska Institutet, Department of Medical Biochemistry and Biophysics, SE-171 77 Stockholm, Sweden
[3]Discovery Genomics, Inc., 614 McKinley Place N.E., Minneapolis, MN 55413, USA
[4]Klinik für Tumörbiologie mbH, Breisacherstrasse 117, D79106 Freiburg, Germany
[5]Department of Medical Biochemistry, Göteborg University, SE-405 30 Göteborg, Sweden
[6]Department of Genetics, Development and Cell Biology, 503 Science II, Iowa State University, Ames, IA 50011, USA
[7]These authors contributed equally to this work
[8]Present address: Göteborg University, SE-405 30 Göteborg, Sweden
[9]Present address: Yorktown Technologies, Plant City, FL 33565
[10]Present address: Cellartis AB, SE-413 46 Göteborg, Sweden
[11]Present address: Qamcom AB, SE-421 30 Göteborg, Sweden
[12]Present address: University of Minnesota, Minneapolis, MN 50011
[13]Present address: SurModics, Inc., Eden Praire, MN 55344
[14]Present address: Unilabs, SE-405 22 Göteborg, Sweden
[15]Present address: Mayo Clinic, Rochester, MN 55905
[16]Present address: Lund Univeristy, SE-221 00 Lund, Sweden
[17]Present address: ProQinase GmbH, D-79106 Freiburg, Germany
[18]Present address: DKFZ, D-69120 Heidelberg, Germany
*Correspondence: mats.hellstrom@ki.se
DOI 10.1016/j.chembiol.2009.02.010

SUMMARY

We combined reverse and chemical genetics to identify targets and compounds modulating blood vessel development. Through transcript profiling in mice, we identified 150 potentially druggable microvessel-enriched gene products. Orthologs of 50 of these were knocked down in a reverse genetic screen in zebrafish, demonstrating that 16 were necessary for developmental angiogenesis. In parallel, 1280 pharmacologically active compounds were screened in a human cell-based assay, identifying 28 compounds selectively inhibiting endothelial sprouting. Several links were revealed between the results of the reverse and chemical genetic screens, including the serine/threonine (S/T) phosphatases *ppp1ca*, *ppp1cc*, and *ppp4c* and an inhibitor of this gene family; Endothall. Our results suggest that the combination of reverse and chemical genetic screens, in vertebrates, is an efficient strategy for the identification of drug targets and compounds that modulate complex biological systems, such as angiogenesis.

INTRODUCTION

Blood vessels allow for the efficient transportation of cells, macromolecules, nutrients, and oxygen to peripheral tissues, and for the removal of carbon dioxide and waste products. Angiogenesis is the formation of new blood vessels from existing ones and is an essential component of both physiological and pathological tissue growth (Adams and Alitalo, 2007). Angiogenesis inhibitors have become important drugs in the treatment of solid tumors and age-related macular degeneration (reviewed by Andreoli and Miller [2007] and Ellis and Hicklin [2008]). Bevacizumab (Avastin), a monoclonal antibody that neutralizes vascular endothelial growth factor A (VEGF-A), was the first FDA-approved therapy selectively targeting angiogenesis (Ferrara et al., 2004). However, Bevacizumab and other angiogenesis inhibitors have several drawbacks; they are only efficient in combination with cytotoxic drugs, there are significant side effects, and tumors may use alternate pathways to evade the effect of VEGF-A blockade (Casanovas et al., 2005; Eskens and Verweij, 2006; Ridgway et al., 2006; Zhu et al., 2007). Thus, there is a need to identify additional angiogenesis targets and develop improved antiangiogenic drugs. Several gene products that are potential drug targets for antiangiogenic applications have been revealed by reverse and forward genetic studies in mice and zebrafish (Adams and Alitalo, 2007; Cha and Weinstein, 2007) . Additionally, chemical genetic screens with in vitro cellular assays or in vivo screens in zebrafish have been employed to identify drugs and drug-like compounds that can modulate angiogenesis (Chan et al., 2002; Kwon, 2006; Tran et al., 2007).

In order to identify genes, known drugs, and pharmacologically active compounds previously not implicated in angiogenesis modulation, we tested the feasibility of running parallel

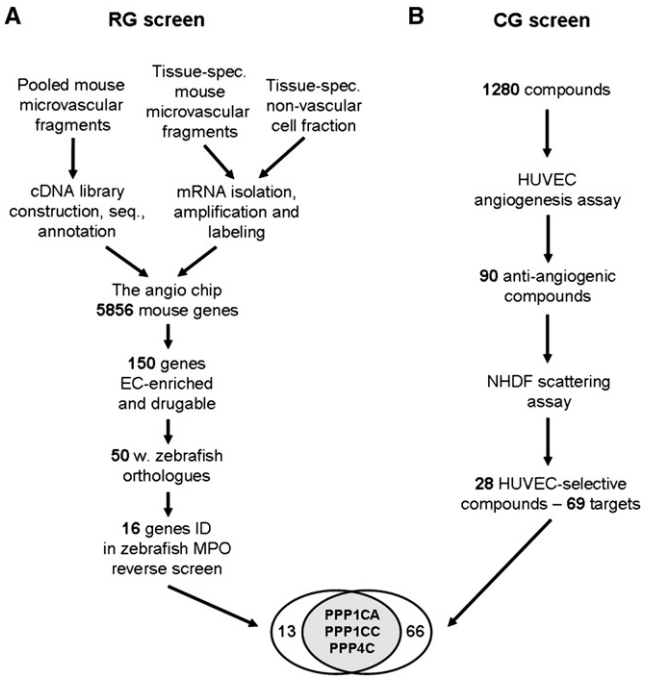

Figure 1. Experimental Overview of the Parallel Reverse and Chemical Genetic Screens

(A) The reverse genetic (RG) screen comprised 5856 genes derived from cDNA libraries, constructed from pooled mouse vascular fragments isolated in vivo. Vascular and corresponding nonvascular samples from various tissues and stages were isolated and underwent RNA extraction, amplification, and labeling. After mRNA expression profiling, 150 mouse genes were selected for functional validation. Fifty mouse genes had suitable zebrafish orthologs, and their functional importance in angiogenesis was evaluated by morpholino-mediated knockdown in zebrafish embryos. Sixteen of the 50 knockdowns resulted in vascular defects.

(B) In a separate chemical genetic (CG) screen, 1280 compounds were screened in a human cellular angiogenesis assay. Ninety compounds inhibited in vitro angiogenesis, and 28 of these, targeting 69 proteins, did not affect fibroblast scattering. At the intersection of the two screens, three genes encoding members of the PPP1 and PPP2 families of S/T phophatases were identified as angiogenesis targets.

reverse genetic (RG) and chemical genetic (CG) screens, taking advantage of several different vertebrate model systems. Our hypothesis was that functionally important targets and pathways will be conserved between species, and will therefore be represented in several different models. Thus, identification of overlapping gene products in the RG and CG screens would serve to reduce the noise and possibly reflect drug targets and/or pathways that are fundamental for angiogenesis.

We used transcript profiling in mice to identify 150 potentially druggable microvessel-enriched gene products. Orthologs of 50 of these were identified and verified by using Ensembl or the National Center for Biotechnology Information's HomoloGene and were knocked down in a RG screen in zebrafish, demonstrating that 16 were necessary for developmental angiogenesis. In parallel, we screened 1280 pharmacologically active compounds in a human cell-based assay, identifying 28 compounds selectively inhibiting endothelial sprouting. The mouse provided us with a well-studied mammalian system with close homology to humans. The zebrafish offers several advantages for RG screening of angiogenesis-modulating genes, including its rapid development that can be followed noninvasively over time. Lastly, as the goal is to develop compounds for human targets and diseases, we used a human cell assay for the CG screen.

Our results support the notion that the combination of RG and CG screens, in vertebrates, is an efficient strategy for the identification of drug targets and compounds that modulate complex biological systems, such as angiogenesis.

RESULTS

Reverse Genetic Screen for Novel Angiogenesis Targets

The first step when selecting genes for the RG screen was to identify genes expressed in the vasculature, i.e., endothelial cells, pericytes, and/or smooth muscle cells. We reasoned that genes with high or selective expression in these cell types would have an increased likelihood of being required for angiogenesis. In addition, an enriched expression in the vasculature could potentially make them specific angiogenesis targets with fewer side effects. We identified vascular-enriched genes by mRNA expression profiling of isolated vascular fragments as well as nonvascular cells from developing and adult mouse tissues. We chose to use mice because vascular fragments can be isolated in sufficient quantities directly from the tissue with minimal perturbation of gene expression, and close similarities exist between the mouse and human genomes. Specifically, we searched for genes that were (i) generally enriched in vascular fragments; (ii) expressed in a particular vascular bed; and/or (iii) expressed preferentially in either developing or adult vasculature. The expression profiling was performed by using custom cDNA arrays constructed from cDNA libraries from vascular fragments. The array contained 12,554 EST clones, representing 5856 unique genes, and was estimated to cover approximately half of the microvascular transcriptome. Importantly, genes known to be expressed in the vasculature, such as the vascular endothelial cadherin (ve-cadherin/*cdh5*) and *endoglin*, were overexpressed in vascular preparations compared to nonvascular cells (Figure 1; see Figures S1 and S2 available online).

Genes were selected for further analysis based on microvascular-enriched expression, as determined by microarray experiments; the presence of signal peptides and/or a transmembrane motif, according to Ensembl annotation; druggability, as predicted by Gene Ontology annotation; and literature searches (Figure S3; Tables S1 and S2). In summary, this resulted in the selection of 150 mouse genes. Through comparison with a reference set of 58 genes with known selective expression in the vasculature (Wallgard et al., 2008), we estimated that the selection process resulted in a more than 20-fold enrichment of genes with a vascular expression (Supplemental Experimental Procedures).

To assess gene function in a semi-high-throughput fashion, we chose to knock down the gene products in zebrafish, by injection of antisense morpholino oligonucleotides (MPOs). This approach allowed for a rapid assessment of the requirements of these genes during angiogenesis in a whole organism. First, zebrafish orthologs of the selected genes were identified by using BLAST searches of zebrafish cDNA and genomic sequence databases. A total of 62 zebrafish orthologs representing 50 mouse genes were identified with a sufficient 5′ UTR sequence to allow for

Table 1. Gene Products Identified by mRNA Expression Profiling in Mice and Reverse Genetics in Zebrafish

		mRNA Expression Profile			Functional Validation	
Gene Name	Gene Ontology Molecular Function	Vascular Selectivity	Pref. Vasc. Bed	Pref. Stage	*cdh5* ISH	FITC-Dextran
alox5ap	Enzyme activator activity	Yes	Skin	-	0%	48%
ctsz	Cysteine-type peptidase activity	Yes	-	-	12%	19%
fzd6	G protein-coupled receptor activity	Yes	-	-	21%	55%
gnb2l1	GTPase activity	Yes	-	Embryo	12%	49%
hexb	β-N-acetylhexosaminidase activity	Yes	Brain	Adult	28%	58%
kiaa1274	Protein tyrosine phosphatase activity	Yes	Brain	Embryo	10%	53%
p2ry5	Purinergic receptor activity, G protein coupled	Yes	Skin	Adult	20%	24%
ppap2a	Phosphatidate phosphatase activity	Yes	-	Adult	48%	57%
ppih	Cyclosporin A binding	Yes	Heart	Embryo	3%	82%
ppp1ca	Protein Ser/Thr phosphatase activity	Yes	-	Embryo	0%	81%
ppp1cc	Protein Ser/Thr phosphatase activity	No	Brain	-	32%	44%
ppp4c	Protein Ser/Thr phosphatase activity	Yes	Heart	Embryo	18%	28%
rab11a	GTPase activity	Yes	Heart	Adult	0%	32%
rab5c	GTPase activity	Yes	Skin	-	0%	54%
ralb	GTP binding	Yes	-	Embryo	12%	84%
sat1	Diamine N-acetyltransferase activity	Yes	Heart	Embryo	0%	43%

All gene names are for human genes. Vascular selectivity was defined as "Yes" or "No," where "Yes" corresponded to upregulated ($p < 0.05$) signal in one or more comparisons of vascular fragments against nonvascular tissues, and "No" corresponded to nonregulated signal in one or more comparisons of vascular fragments against nonvascular tissues. Preferentially enriched expression in a vascular bed (Pref. Vasc. Bed) was defined as upregulated ($p < 0.05$) signal in one vascular bed compared to another vascular bed. Significantly higher expression of a gene at embryonic or adult stages was indicated as either preferred "Embryo" or "Adult." The underlying data are presented in Table S2. *cdh5* ISH, the percentage of zebrafish embryos with aberrant *cdh5* expression in the intersegmental vessels at 48–56 hpf, as detected by in situ hybridization. FITC-Dextran, the percentage of zebrafish embryos with defective intersegmental vessels evident by FITC-dextran microangiography at 48–56 hpf. Details of reduced *cdh5* staining and/or FITC-dextran labeling are shown in Figure S4.

the construction of suitable MPOs (Tables S2–S4). These 62 genes were knocked down in zebrafish embryos by microinjection of at least two different MPOs for each gene into 1-cell zebrafish embryos. To control for nonspecific effects as a result of MPO injection, two nonoverlapping MPOs were used for each gene. Dose-response experiments were carried out for each MPO individually and in combination. In addition, injection of a mixed-base MPO had no effect on vascular development, even at a high dose (Figure 4). The zebrafish embryos were analyzed at 24 and 56 hr postfertilization (hpf) for alterations in vascular development. Selection criteria in the primary screen comprised visually detectable defective blood flow and/or reduced intersegmental vessel (ISV) sprouting detected as reduced *cdh5* staining in the vessels at 48–56 hpf. Knockdown embryos exhibiting either of those changes were analyzed in MPO dose-response studies and analyzed in detail for *cdh5* mRNA expression at 24 and 56 hpf by mRNA in situ hybridization. The embryos were also subjected to microangiography by using fluorescent dextran injection at 48–56 hpf. Heart beat was monitored to exclude heart dysfunction as an explanation for reduced vascular perfusion. Sixteen genes exhibited significant dose-dependent vascular defects in response to both injected MPOs (Table 1; Figure S4; Table S5). For one of them, *rab5c*, vascular leakage was also detected as extravasation of fluorescent dextran (Figure S4I). Interestingly, several phosphatases were identified in the RG screen. Three of the 16 genes were S/T phosphatases (*ppp1ca*, *ppp1cc*, and *ppp4*), and one was a predicted tyrosine phosphatase (kiaa1274, mouse ortholog x99384).

We performed mRNA in situ hybridization on mouse embryo tissue to validate the gene expression of the 16 genes identified in the RG screen. Four out of 16 genes were selectively expressed in vascular cells: *sat1*, *ppap2a*, *x99384*, and *fzd6* (Figures 2A–2D; Figure S5 [Visel et al., 2004]). The other 12 genes, including 3 S/T protein phosphatases, *ppp1ca*, *ppp1cc*, and *ppp4c*, were overexpressed in vascular cells, but were also expressed in other cell types (Figures 2E–2G, and data not shown).

Chemical Genetic Screen for Novel Angiogenesis Drugs and Targets

We screened 1280 well-characterized compounds from the List of Pharmacologically Active Compounds (LOPAC^{1280}) in a cellular angiogenesis assay (Korff and Augustin, 1998). We chose this chemical library, as the compounds have partially, to extensively, characterized targets. The assay evaluates the effect of compounds on angiogenic sprouting of human umbilical vein endothelial cells (HUVECs), stimulated with VEGF-A in a three-dimensional collagen type I matrix (Figures S6A–S6D). The effect was determined as percentages of the positive VEGF-A control, which was set to 100%. In the primary screen, 90 inhibitory compounds were identified via microscope observation by two independent observers. These compounds were rescreened, and their inhibitory effects on sprouting were quantified. To assess endothelial selectivity, the set of 90 compounds were subsequently assayed for their effects on fibroblast scattering by using normal human dermal fibroblasts (NHDFs). Twenty-eight compounds, known to interact with 69 targets, showed

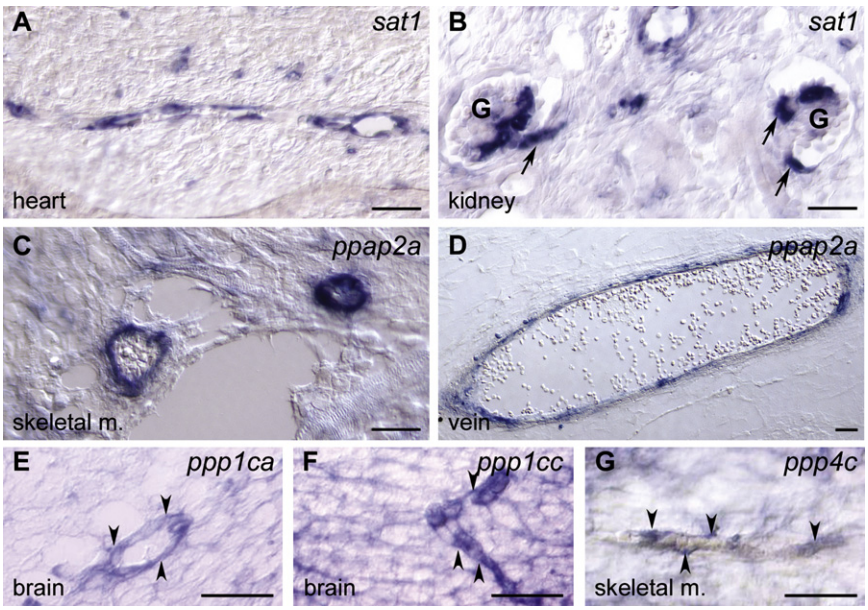

Figure 2. Validation of Vascular Expression of Gene Products Identified in the Reverse Genetic Screen

(A–G) Gene expression determined by nonradioactive mRNA in situ hybridization (blue) on mouse tissues. (A) *sat1* expression was restricted to the microvasculature in the heart at embryonic day (E) 17.5. (B) Expression of *sat1* in the vasculature of kidney glomeruli (G) at E17.5. Arrows indicates afferent and efferent arterioles. (C and D) At E17.5, *ppap2a* was mainly expressed in large vessels, here exemplified by two vessels in skeletal muscle (skeletal m.) and a vein (vein). (E–G) The S/T protein phosphatases *ppp1ca*, *ppp1cc*, and *ppp4c* were all expressed in the vasculature as well as in other cell types. (E) Vascular *ppp1ca* staining in the brain at E17.5 (arrowheads). (F) Vascular expression of *ppp1cc* in the brain at E14.5 (arrowheads). (G) Vascular expression of *ppp4c* in skeletal muscle at E17.5 (arrowheads). Scale bars represent 100 μm.

significant inhibition of endothelial sprouting (<50% of VEGF-A-induced sprouting), yet left fibroblast scattering relatively unaffected (>50% of NHDF control scattering) (Figure 3; Table S6).

As expected, the screen identified compounds already known to inhibit angiogenesis. For example, among the 90 antiangiogenic compounds we found the tyrosine kinase inhibitor SU5416, designed to selectively inhibit VEGFR2 (Fong et al., 1999), and shown by others to be antiangiogenic in zebrafish (Chan et al., 2002). Furthermore, Nimesulide and β-Lapachone were among the 28 selective compounds. Nimesulide is a highly selective cyclooxygenase-2 inhibitor that belongs to a class of drugs known to inhibit angiogenesis (Tsujii et al., 1998). β-Lapachone, a naphthoquinone compound derived from the bark of the lapacho tree (*Tabebuia avellanedae*), has been shown to have both antitumor activity and antiangiogenic properties (Kung et al., 2007).

Reverse and Chemical Genetic Screens Identify an Overlap of Pathways and Targets

In the sets of 16 genes and 28 compounds, we found several regulators of prostaglandin/leukotriene synthesis, molecules known to affect angiogenesis (reviewed by Romano and Claria [2003]). For example, in the RG screen, we identified *ppap2a*, which converts phosphatidic acid to diacylglycerol. Diacylglycerol is, in turn, converted to arachidonic acid, the

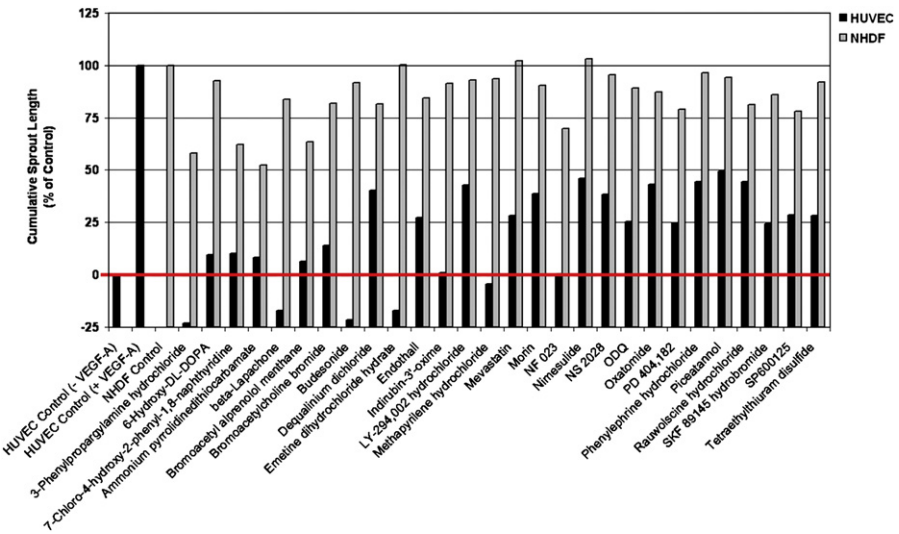

Figure 3. Twenty-Eight Compounds Inhibit VEGF-A-Induced HUVEC Sprouting Angiogenesis

VEGF-A-driven HUVEC angiogenesis was quantified as the average cumulative sprout length (black bars). The VEGF-A-driven sprouting was set to 100%, and the basal sprouting in the absence of VEGF-A was set to 0%. The red line is a reference line for the basal HUVEC sprouting. Scattering of clustered NHDFs in collagen gels in the presence of basal medium was set to 100% (gray bars). Twenty-eight compounds from the LOPAC library inhibited sprouting at > 50% (black bars) and NHDF scattering at < 50% (gray bars).

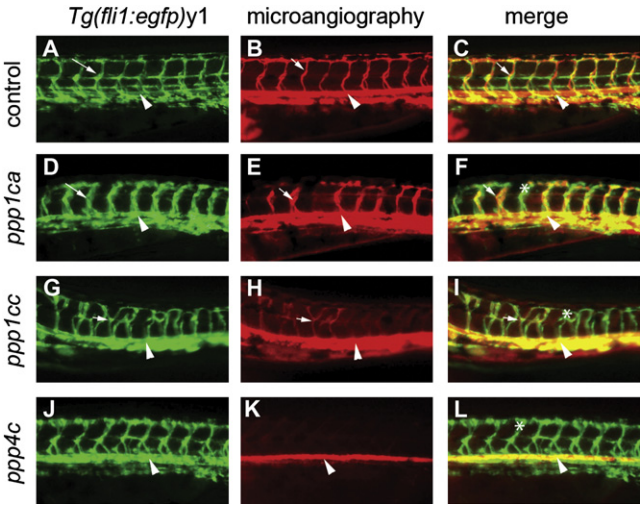

Figure 4. Knockdown of *ppp1ca*, *ppp1cc*, and *ppp4c* Results in Defects in Endothelial Path Finding and Tubulogenesis

(A–L) Images are all lateral views of the trunk vasculature at 48–50 hpf. (A–C) Control embryo injected with a mixed-base morpholino. (D–L) Embryos injected with morpholinos against (D–F) *ppp1ca*, (G–I) *ppp1cc*, and (J–L) *ppp4c*. Endothelial cells (shown with green fluorescence in [A], [D], [G], and [J]) were identified by using the Tg(*fli1:egfp*)^{y1} line. Dorsal aortas are marked with arrowheads, examples of perfused ISVs are marked with arrows, and examples of nonperfused ISVs are labeled with asterisks. (D and J) The *ppp1ca* and *ppp4c* knockdowns resulted in enlarged ISVs, whereas (G) knockdown of *ppp1cc* resulted in excessive branching of the ISVs. (B) At 48–50 hpf, circulation as observed by microangiography was observed in control injected embryos (mixed-base MPO) in the dorsal aorta, cardinal vein, and ISVs. (E and K) Rhodamine-dextran dye (red) often entered the ventral aspect of the ISVs in the *ppp1ca* and *ppp4c* knockdowns (a more severely affected embryo is shown for *ppp4c*), but a circulatory loop was not established. (H) The *ppp1cc* knockdown embryos showed either an absence of circulation or thin vessels with reduced circulation. (C, F, I, and L) Merged images of the embryos shown in the previous two panels.

precursor of both prostaglandins and leukotrienes. Among the 16 targets of the RG screen was *alox5ap*, which converts arachidonic acid to hydroperoxyeicosatetraenoic acid (HPETE), the immediate precursor of leukotriene A4. Furthermore, among the 28 compounds identified in the CG screen, we discovered two compounds inhibiting prostaglandin and leukotriene biosynthesis: Nimesulide, which inhibits the synthesis of prostaglandin from arachidonic acid, and Budesonide, which suppresses the synthesis of both prostaglandin and leukotrienes, via the glucocorticoid receptor (Figure S7).

In light of the identification of 3 S/T protein phosphatases in the RG screen, it was striking that 1 of the 28 compounds, Endothall, is known to inhibit S/T protein phosphatases. There are five known gene families of S/T protein phosphatases: PPP1, PPP2A, PPP3, PPP5, and PPP7 (Cohen, 2004). Endothall inhibits members of the PPP1 and PPP2A families (Erdodi et al., 1995), with PP1 being five times less sensitive than PP2A to Endothall (Li et al., 1993). Out of the S/T protein phosphatases identified in the RG screen, *ppp1ca* and *ppp1cc* belong to the PPP1 family, and *ppp4c* belongs to the PPP2A family (Cohen et al., 2005; Cohen, 2004). Thus, three genes that were identified in the RG screen corresponded to two of the gene families identified in the CG screen (Figure 1).

There were three other S/T phosphatase inhibitors present among the 1280 compounds screened: the PPP1 and PPP2A family inhibitors Cantharidin and Cantharidic acid (both structural analogs of Endothall), as well as Cyclosporin A (a PPP3-family inhibitor). Cantharidin and Cantharidic acid were present among the 90 identified antiangiogenic compounds. However, at the screening concentration used, these compounds also affected fibroblast scattering, and were thus excluded in the process. Cyclosporin A had no effect on angiogenic sprouting (data not shown), further suggesting specificity to the involvement of PPP1 and PPP2A family members in angiogenesis.

Protein Phosphatases *ppp1ca*, *ppp1cc*, and *ppp4c* Affect Vascular Perfusion

We next focused on the S/T protein phosphatases that overlapped in the two screens. First, we performed a dose-response titration of Endothall in the cellular angiogenesis assay. This resulted in IC_{50} values for HUVECs and NHDFs of 0.25 μM and 1.2 μM, respectively, thus indicating that endothelial cells are five-fold more sensitive to PPP1 and/or PPP2A inhibition than NHFDs (Figures S6E and S6F). Second, to better characterize the effects observed in the RG screen, we repeated the zebrafish knockdown experiments with *ppp1ca*, *ppp1cc*, *ppp4c*, and control MPOs in a transgenic line of zebrafish expressing green fluorescent protein in endothelial cells, Tg(*fli1:egfp*)^{y1}. These transgenic embryos allowed us to follow endothelial migration during embryonic vasculogenesis and angiogenesis. Subsequent formation of patent perfused vessels was assessed by using microangiography at 48–50 hpf.

In all S/T protein phosphatase knockdowns, microangiography revealed defects in perfusion (Figure 4; Table 2). The endothelial cells that form the axial vasculature migrated to the midline, and sprouting from this location to form the ISVs appeared to be normal. However, in the most severely affected embryos of *ppp1cc* knockdowns, the ISVs displayed excessive branching, although the endothelial cells were able to migrate dorsally. This path-finding phenotype is similar to the knockdowns of the neuropilins in zebrafish (Martyn and Schulte-Merker, 2004). For knockdown of *ppp1ca* and *ppp4c*, incomplete perfusion was accompanied by a dilated or enlarged vessel diameter (J.J.E., unpublished data). Based on the phenotypes observed after gene knockdown, the protein phosphatases *ppp1ca*, *ppp1cc*, and *ppp4c* may thus have roles during both endothelial guidance and tubulogenesis/perfusion. The PPP1 and PPP2A gene families have many targets and have been implicated in numerous cellular functions (reviewed by Cohen [2002, 2004] and Cohen et al. [2005]). They are highly conserved and homologous, which suggests a high degree of functional redundancy. However, the vascular defects in otherwise overtly normal S/T protein phosphatase knockdown embryos indicate specific functions or particular sensitivity to protein phosphatase-regulated signaling in the vasculature.

Endothall Treatment of Zebrafish Phenocopies the Knockdowns of *ppp1ca*, *ppp1cc*, and *ppp4c*

Next, we were interested to test whether treatment with Endothall, the S/T phosphatase inhibitor identified in the chemical screen, would result in similar phenotypes as the knockdowns of the S/T protein phosphatases. Zebrafish embryos were

Table 2. Analysis of Vascular Defects from the Knockdown of *ppp1ca*, *ppp1cc*, and *ppp4c*: Analysis by Microangiography in the Tg(*fli1:egfp*)^{y1} Zebrafish Line

				ISV Defects				
		Axial Vascular Defects		ISV Defects in Total				
Condition	MPO Dose	%	n	%	n	Low %	Medium %	High %
Control		2%	49	10%	43	0%	0%	10%
Control MPO	6 ng	0%	11	0%	11	0%	0%	0%
	12 ng	0%	9	0%	9	0%	0%	0%
ppp1ca	12 ng	0%	10	50%	10	20%	10%	20%
ppp1cc	4.5 ng	7%	15	86%	14	50%	21%	14%[a]
	9 ng	25%	12	89%	9	22%	44%	22%[a]
ppp4c	4 ng	48%	23	83%	12	8%	8%	67%
	4 ng	7%	14	15%	13	15%	0%	0%
	8 ng	60%	15	17%	6	0%	0%	17%
	8 ng	0%	9	44%	9	33%	11%	0%

Tg(*fli1:egfp*)^{y1} embryos were injected with morpholinos against *ppp1ca*, *ppp1cc*, or *ppp4c*. Vascular development was scored at 48–50 hpf by examining circulation using microangiography and accessing endothelial migration after EGFP fluorescence. Axial vascular defects were scored as an absence of circulation in the dorsal aorta and cardinal vein. These embryos could not be examined for circulation in the ISVs. Defects in the circulation in the ISVs were scored as low (<30% affected), medium (30%–70% affected), or high (>70% affected).
[a] Pathfinding defects of the endothelial cells in the ISVs were observed after the knock down of *ppp1cc* in the highly affected class.

soaked in different concentrations of Endothall, and treatment was initiated at the 20-somite stage (equivalent to 20 hpf). During this stage, the axial vessels in the trunk, the dorsal aortal, and the cardinal vein form by vasculogenesis and begin tubulogenesis. Also, at the same time, the first wave of angiogenesis from the dorsal aorta begins as endothelial cells migrate to form the ISVs. Using a similar strategy as for the analysis of the knockdown phenotypes described above (Figure 4), endothelial migration during formation of the ISVs was followed in the Tg(*fli1:egfp*)^{y1} transgenic embryos, and the emergence of patent vessels was investigated by using microangiography at 48–50 hpf. Similar to knockdowns of *ppp1ca*, *ppp1cc*, and *ppp4*, Endothall treatment resulted in dose-dependent reduction of ISV perfusion without strongly affecting endothelial migration (Figure 5).

DISCUSSION

To our knowledge, this is the first systematic study combining parallel RG and CG screens in vertebrates. CG screens are powerful tools in research and drug discovery, but they are hampered by the difficulty of identifying the targets of the effective compounds. In invertebrates, it has been shown that a comparison between phenotypes resulting from RG and compound screens in the same model system may reveal targets or pathways affected by the compound. For example, in *Drosophila*, phenotypic comparison showed that γ-secretase inhibitors target the NOTCH receptor, and in *Caenorhabditis elegans*, Ezetimibe was shown to target the *annexin2* pathway (Ross-Macdonald, 2005). Moreover, the use of systematic RG and CG screening in *Drosophila* has linked new drug-like compounds to known pathways that control specific biological processes, such as cytokinesis (Eggert et al., 2004). However, from a drug development perspective, invertebrate model systems have limitations both in the types of biological processes that may be assayed, and in their relevance to human disease. For example, limitations are apparent when diseases that affect the vascular system are considered. Many of the known signaling pathways in the vascular system of vertebrates are not represented in invertebrates, nor are well-developed circulatory systems. Our results suggest that parallel RG and CG screens can be used, not only in invertebrates, but also in more complex, and for human disease, more relevant vertebrate systems, to identify candidate targets/pathways hit by to compounds having an effect in chemical screens. Larger screens and applications in other areas than angiogenesis are clearly needed to validate whether the combination of RG and CG screens in vertebrates commonly identify the same targets and processes, but our study does suggest that this may very well be the case.

The task of identifying the overlap of the screens was simplified because the targets of the compounds used in the CG screen have previously been partly characterized. This is not the case when large libraries containing new chemical entities are tested. However, the fact that Endothall phenocopied the knockdowns of *ppp1ca*, *ppp1cc*, and *ppp4c*, and that we identified key components of the prostaglandin/leukotriene biosynthesis pathway in both screens, suggest that detailed phenotypic comparison of RG and CG screens can reveal which targets or pathways are also affected by novel chemical entities.

Obviously, an important question is whether the assays score for the same biological process. In the CG screen, the readout is inhibition of endothelial sprouting, and in the RG screen we screen for both angiogenesis and perfusion defects. In the CG screen, we identified Endothall as a compound with inhibitory effects on endothelial sprouting. However, when we knock down the expression of its target genes, including *ppp1ca*, *ppp1cc*, and *ppp4cc*, we primarily detect a defect in vascular perfusion, but not in endothelial migration. We believe that the underlying mechanism triggering the different outcomes might be the same, but depending on the specific assay or model, they will result in different phenotypes. This has been observed

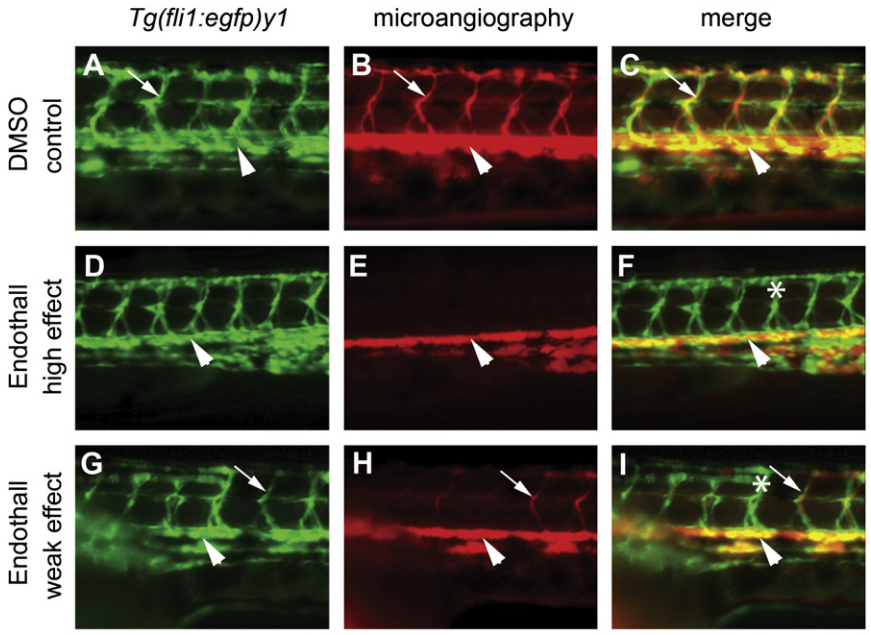

J	Control	Endothall Concentration		
	1% DMSO	650 uM	750 uM	950 uM
Axial Vessel Defects	0%	25%	14%	100% Vascular Collapse
ISV Defects	33%	78%	83%	
ISV Defects - Low	17%	33%	33%	
ISV Defects - Medium	0%	22%	17%	
ISV Defects - High	17%	22%	33%	
Total Vessel Defects	33%	83%	86%	

Figure 5. Treatment of Embryos with Endothall Results in Defects in Tubulogenesis

(A, D, and G) Endothelial cells in the trunk were analyzed for defects in migration in the *Tg(fli1:egfp)*^{y1} line (green fluorescence) at 48–50 hpf. (B, E, and H) Analysis of circulation defects by using microangiography (rhodamine-dextran imaging, red) at 48–50 hpf. (A–I) are lateral views of the trunk. (A–C) Treatment with either carrier (DMSO control) or (D–I) Endothall did not alter endothelial migration (see *Tg(fli1:egfp)*^{y1} in [A], [D], and [G]). (B, E, and H) Microangiography revealed defects is circulation consistent with defects in tubulogenesis. Two classes of affected embryos are shown. In weakly affected embryos (low effect), some of the ISVs would fail to circulate rhodamine-dextran. In more severely affected embryos (high effect), most of the ISVs failed to transfer dye. (C, F, and I) Merged images of the previous two panels. Dorsal aortas are marked with arrowheads, examples of perfused ISVs are marked with arrows, and examples of non-perfused ISVs are labeled with asterisks. (J) Dose response to bathing embryos in Endothall. Embryos were scored based on circulation in the axial vessels and the ISVs as in Table 2. Vascular collapse was observed with the highest concentration of Endothall.

before when studying the same gene in different models. For example, the mouse knockout of *vegfr2* results in early embryonic lethality due to a halt in vasculogenesis and angiogenesis (Shalaby et al., 1995). However, the knockdown of *vegfr2* in zebrafish displays flow defects (Bahary et al., 2007). Importantly, it is clear from both of these studies that *vegfr2* has an important role in blood vessel development. Needless to say, results from a screen must be interpreted carefully, and more studies are required to confirm and extend the analysis in order to mechanistically understand the results of these initial findings.

The LOPAC set of 1280 compounds contained 4 S/T protein phosphatase inhibitors in total. Three PPP1 and PPP2A inhibitors, Cantharidin, Cantharidic acid, and Endothall, were among the set of 90 antiangiogenic compounds identified. The fourth inhibitor was Cyclosporin A, a PPP3-family inhibitor that was not identified by the screens, suggesting that PPP1 and PPP2A, but not PPP3, have roles in vascular development. Cantharidin and Cantharidic acid were excluded from the final hit list, not because they were not efficient antiangiogenic compounds, but rather because they also had an inhibitory effect on fibroblast scattering. Importantly, Cantharidin and Cantharidic acid are ~10-fold more potent inhibitors of PPP1 and PPP2A than Endothall. Thus, at the screening concentration used, any selective sensitivity of HUVECs (compared to NHDFs) to Cantharidin and Cantharidic acid is likely masked by the potency of these compounds, enabling them to affect NHDFs as well.

The PPP1/PPP2A inhibitor Endothall and its structural analogs are compounds with an inherent and increasing toxicity in the following sequence: Endothall < Cantharidic acid < Cantharidin (Li et al., 1993). In our experiments, in which zebrafish embryos were treated with Endothall, the effective dose was close to the toxic dose. This finding is supported by studies of Cantharidin in mice by others (Eldridge and Casida, 1995; Wang, 1989). Nevertheless, there are several lines of evidence that suggest that members of the PPP1 and PPP2 families have specific roles in vascular formation. First, morpholino knockdowns of *ppp1ca*, *ppp1cc*, and *ppp4* are selective, and each results in vascular defects in morphologically overtly normal embryos (Figure 4; Figures S4K, S4L, and S4O). Second, the IC_{50} titration of Endothall indicates that endothelial cells are more sensitive than NHDFs. Third, the effect of Endothall on vascular perfusion in zebrafish was dose dependent and effective at a lower than toxic dose. In summary, this argues for a primary role of the PPP1 and PPP2A families of S/T phosphatases in proper vascular formation.

The fact that two independent screens identified S/T protein phosphatases from the PPP1 and PPP2A families suggests that these genes are critically involved in angiogenesis. Our findings are strengthened by the fact that we arrive at the same targets from screening approaches involving different species and models. Future studies will address the mechanisms behind the effects of the PPP1 and PPP2A families of S/T phosphatases on blood vessels. Potential mechanisms for the PPP1 family include modulation of vascular permeability, cytoskeletal structure, and filopodia extension. PPP2A has been implicated in endothelial migration (Hartel et al., 2007; Li et al., 2007; Shinoki

et al., 1995; Young et al., 2002). Moreover, Cantharidin, the 2, 3-dimethylanhydride of Endothall, has been shown to enhance endothelial-mediated contraction of arteries and endothelial permeability (Knapp et al., 1999, 2000). We thus note that the cell biological roles of the PPP1 and PPP2A families, to a certain extent, overlap those of VEGF-A, and we are currently investigating the relationship of these genes to the VEGF pathway (J.J.E., unpublished data). Another major signaling pathway in vascular biology is TGF-β (reviewed by Gaengel et al. [2009]), affecting many different steps in angiogenesis, including lumen formation (Oh et al., 2000). It is therefore interesting that PP1α determines the duration of TGF-β signaling (Valdimarsdottir et al., 2006). Furthermore, the PPP1 and PPP2A inhibitor Cantharidin, historically extracted from the blister beetle, *Mylabris phalerata*, has been used in traditional medicine as an antitumoral substance for thousands of years. When tested in the clinic, Cantharidin was shown to have beneficial effects against primary hepatoma (Wang, 1989). It will be important to determine the degree to which these effects on tumorigenesis are attributable to the antiangiogenic properties of PPP1 and PPP2A inhibitors shown in this study.

SIGNIFICANCE

Inhibition of angiogenesis is an important mode of action for several oncology drugs on the market, but there is still a need to find new drugs to obtain greater efficacy and fewer side effects. We show that parallel reverse genetic (RG) and chemical genetic (CG) screens complement each other and facilitate target identification in angiogenesis. Thereby, we identify 16 putative drug targets and 28 pharmacologically active compounds, targeting 69 gene products, all with angiogenesis-regulating properties. Importantly, we identify an overlapping set of targets and pathways from the two screening approaches. To our knowledge, this is the first report describing the use of parallel RG and CG in vertebrates to identify and validate drug targets and pathways.

EXPERIMENTAL PROCEDURES

RNA Preparation and cDNA Library Construction

Isolation of mouse microvascular fragments by using Dynabeads (Dynal, Invitrogen) has been described previously (Bondjers et al., 2006). In this study, microvascular fragments were isolated from adult brain and liver and from embryonic (E16.5–18.5) brain, liver, and skin from wild-type, Tie-1 knockout, PDGF-B knockout, and PDGF-Rβ knockout embryos. Protocols were optimized by using Tie2LacZ mice, a knockin mouse in which the endothelial cells can be stained with X-Gal. Using RNeasy mini kits (QIAGEN), 300 mg vascular total RNA was isolated. The RNA was used to produce a standard oligo-dT-primed cDNA library (Soares et al., 1994) (custom synthesis by Incyte). In addition, three normalized libraries were generated from the standard library by using a modification of the technique described by Soares et al. (1994), in which high-abundance transcripts were suppressed to different degrees. In total, the four libraries comprised 16,000 cDNAs cloned into the pBluescript vector and stored as bacterial clones. For descriptions of subsequent sequence trimming and annotation, please see Supplemental Experimental Procedures.

Microarray Data Generation

For a description of the production of spotted cDNA microarrays (the Angio chip), please see Supplemental Experimental Procedures.

Mouse microvascular fragments and the corresponding nonvascular tissue from embryonic (E18.5) heart and skin, adult brain, and adult heart were prepared as previously described (Bondjers et al., 2006). After the separate isolation of total RNA from these cell fractions, the RNA was amplified for two rounds (Scheidl et al., 2002; Wang et al., 2000), in parallel with Universal Mouse Reference RNA (Stratagene). Amplified sample RNA was labeled with the fluorescent dye Cyanine-3 (Cy3) conjugated to UTP (Amersham-Pharmacia, now GE Healthcare), and the Universal Mouse Reference was labeled with Cyanine-5 (Cy5) conjugated to UTP. Cy3- and Cy5-labeled materials were simultaneously hybridized to the Angio chip, by using the DIG Easy Hyb hybridization solution (Roche). Hybridizations were performed in a water bath for 1.5 hr at 44°C, instantly followed by 15–20 hr at 40°C. Hybridized microarrays were washed and thereafter scanned by using a dual laser scanner (GenePix 4000B, Axon). Raw data were extracted by using ImaGene (BioDiscovery) and were processed and normalized with the LOESS method by using the Bioconductor Limma Package (version 2.9.11, www.bioconductor.org).

Mouse mRNA In Situ Hybridization

Nonradioactive mRNA in situ hybridization was performed on 14 μm thick sections with digoxygenin-labeled RNA probes (Boehringer Ingelheim) visualized by alkaline phosphatase-conjugated antidigoxygenin antibodies, as described previously (Bostrom et al., 1996). Antisense and sense probes for the investigated genes were generated from the corresponding EST clones of the vascular cDNA libraries through restriction, followed by transcription, with T7 and T3 RNA polymerases.

Zebrafish Experiments

Morpholino design and injection were carried out as described (Nasevicius and Ekker, 2000). For each gene, two nonoverlapping morpholinos were designed against the 5′UTR to the first 25 bp of coding sequence and injected individually and together. When two zebrafish orthologs were found that corresponded to one mouse gene, the overlapping requirements of both genes during vascular development were tested in double knockdown experiments. In situ hybridization with *cdh5* was conducted as described (Larson et al., 2004) with ~40 embryos that were coinjected with two morpholinos. Morpholino doses that resulted in severe cell death were avoided (Ekker, 2000). To control for nonspecific effects as a result of MPO injection, two nonoverlapping MPOs were used for each gene, and dose-response curves were carried out for each MPO individually and in combination. Forty-six of the genes targeted with MPOs had little or no effect on vascular development, suggesting specificity for the 16 genes we identified as being required for vascular development. In addition, injection of a mixed-base MPO had no effect on vascular development, even at a high dose. Microangiography was performed by using FITC or rhodamine-dextran injection into the sinus venosus (Nasevicius and Ekker, 2000). Both in situ hybridization and microangiography experiments were scored by examining endothelial migration and circulation in the intersegemental vessels.

For injection experiments, 3 μl of a solution containing Endothall in 0.5% DMSO was injected directly into the yolk of dechorionated 20-somite-stage Tg(*fli1:egfp*)^{y1} embryos. For bathing experiments, dechorionated embryos were incubated with different concentrations of Endothall in fish water containing 0.5% DMSO. Embryos were raised to 48–50 hpf in plastic petridishes with a 1% agarose pad. Microangiography was performed by injection of 2–5 μl 5 mg/ml rhodamine-dextran (1,000,000 MW, Invitrogen). Fluorescence was observed on a Zeiss Discovery dissection scope. Vascular defects were categorized as normal, low (i.e., <30% absence of intersegmental vessel staining or FITC-dextran signal), Medium (i.e., 31%–70% defective intersegmental vessel staining/signal), or high (i.e., >70% defective intersegmental vessel staining/signal).

Chemical Genetic Screen

LOPAC$_{1280}$ (Library of Pharmacologically Active Compounds) is a collection of chemical compounds that contains marketed drugs, failed development candidates, and "gold standards" that have well-characterized activities (Sigma-Aldrich, Inc.). The LOPAC compounds were tested at a concentration of 10 μM to evaluate their potential to inhibit VEGF-stimulated sprouting of endothelial cells clustered in a three-dimensional gel. Test substances were

stored at −20°C and thawed prior to use. Test substances (10 mM) were diluted to a 10-fold concentrated working solution (100 μM) in endothelial cell basal medium with 25 ng VEGF/100 μl for the stimulation of HUVEC sprouting or without VEGF for assaying fibroblasts.

Compounds were tested as described by Korff and Augustin (1999). In brief, spheroids were prepared by pipetting 500 cells (HUVEC, PromoCell, Heidelberg, Germany) or fibroblasts (NHDF, PromoCell) in a hanging drop on plastic dishes to allow for overnight spheroidal aggregation. Spheroids were harvested, and 50 spheroids were seeded in a solution of 900 μl methocel-collagen and pipetted into individual wells of a 24-well plate to allow collagen gel polymerization. Samples were added after 30 min by pipetting 100 μl of a 10-fold concentrated working dilution of the test substances on top of the gel. Plates were incubated at 37°C for 24 hr. Dishes were fixed at the end of the experimental incubation period by the addition of 1 ml 10% paraformaldehyde.

In the primary screen, the sprouting intensity of endothelial cells was assayed microscopically by two independent investigators. In a rescreen, the sprouting intensity of endothelial cells and fibroblasts was quantified by a semiautomated image-analysis system. The cumulative sprout length per spheroid was determined by using an Olympus IX50 inverted microscope and the digital imaging software analySIS (Soft Imaging System, Münster, Germany). The mean of the cumulative sprout length of ten randomly selected spheroids in each well was analyzed and used as an individual data point. The reductions in angiogenic sprout length were expressed as percentages of the positive VEGF-A control, which was set to index 100. For each plate, baseline control sprouting was measured and subtracted from the measured value of sprout length to ensure valid measurement of VEGF-A-induced sprouting. Thus, the reduction of sprout length (percentage of VEGF-A-induced control) may occasionally give values below zero. The inhibitors were classified according to the following: category 1, inhibition of VEGF-induced HUVEC sprouting (<80% of control sprouting), with a limited effect on fibroblast scattering (>50% of control); category 2, HUVEC sprouting < 50% of control, and fibroblast scattering > 50% of control; category 3, HUVEC sprouting < 50% of control, and fibroblast scattering < 50%; category 4, HUVEC sprouting > 50% of control. A cutoff was set at category 2; thus, only compounds in categories 1 and 2 were included in the list of the 28 selective antiangiogenic compounds. The HUVEC spheroids display minor sprouting activity without the presence of VEGF-A (Figure 4A), which represents the baseline.

Statistical Analysis

At least three biological replicates were used for every cell fraction (e.g., adult brain EC) tested. RNA was isolated from all cell fractions, and each sample was subsequently used for one individual microarray hybridization. The average expression value was calculated for each gene in every sample group (e.g., adult heart EC or embryonic heart EC). The fold change of each gene between the two sample groups was calculated as the ratio between the two averages. To assess the significance of differential expression, a Student's t test was performed on each gene to obtain the raw p value (two-sided, equal variance) (Cui and Churchill, 2003). Multiple test correction of raw p values was done by using the false discovery rate method (Hochberg, 1995). The calculation was performed by using the stats package in R (version 2.4.1, www.r-project.org). Genes with a raw p value $\leq$ 0.05 and a log2 ratio $\geq$ 0.3 or $\leq$ −0.3 were considered as significantly regulated.

For the chemical genetic screen, the average sprout length was determined and the confidence interval was calculated at the α level of 0.05. All selected compounds inhibited sprouting by more than 50% of control when using HUVEC spheroids ($p < 0.05$), but less than 50% of control when using NHDF spheroids ($p < 0.05$).

Ethics

The mice and fish used in the experiments described herein were kept in accordance with applicable animal welfare laws and restrictions. The mouse experiments were approved by the Gothenburg Ethical Committee for Animal Research.

ACCESSION NUMBERS

The details of the microarray data discussed here have been deposited in the National Center for Biotechnology Information's Gene Expression Omnibus (GEO, http://www.ncbi.nlm.nih.gov/geo/) and are accessible through GEO Series accession number GSE10035.

SUPPLEMENTAL DATA

Supplemental Data include six figures, six tables, and Supplemental Experimental Procedures and can be found with this article online at http://www.cell.com/chemistry-biology/supplemental/S1074-5521(09)00076-3.

ACKNOWLEDGMENTS

M.K. and M.H. conceived and designed the study. M.K., E.W., J.J.E., P.B.H., and M.H. wrote the manuscript. M.K., E.W., N.A., and M.H. designed and performed the mRNA expression profiling study. A.N., J.D.L., K.J.C., J.J.E., and P.B.H. designed and performed the reverse genetics in zebrafish. E.B., S.A.W., E.N., L.H., and T.S. performed the bioinformatics. L.K.-L. and A.-K.H. performed mouse mRNA in situ hybridizations. H.A., H.W., L.A., and M.H. designed and performed the HUVEC screen. We thank Jo Anne Powell-Coffman for critical reading of the manuscript.

Received: February 18, 2008
Revised: January 26, 2009
Accepted: February 9, 2009
Published: April 23, 2009

REFERENCES

Adams, R.H., and Alitalo, K. (2007). Molecular regulation of angiogenesis and lymphangiogenesis. Nat. Rev. Mol. Cell Biol. *8*, 464–478.

Andreoli, C.M., and Miller, J.W. (2007). Anti-vascular endothelial growth factor therapy for ocular neovascular disease. Curr. Opin. Ophthalmol. *18*, 502–508.

Bahary, N., Goishi, K., Stuckenholz, C., Weber, G., Leblanc, J., Schafer, C.A., Berman, S.S., Klagsbrun, M., and Zon, L.I. (2007). Duplicate VegfA genes and orthologues of the KDR receptor tyrosine kinase family mediate vascular development in the zebrafish. Blood *110*, 3627–3636.

Benjamini, Y., and Hochberg, Y. (1995). Controlling the false discovery rate: a practical and powerful approach to multiple testing. J. Royal Stat. Soc. B (Methodological) *57*, 289–300.

Bondjers, C., He, L., Takemoto, M., Norlin, J., Asker, N., Hellstrom, M., Lindahl, P., and Betsholtz, C. (2006). Microarray analysis of blood microvessels from PDGF-B and PDGF-Rβ mutant mice identifies novel markers for brain pericytes. FASEB J. *20*, 1703–1705.

Bostrom, H., Willetts, K., Pekny, M., Leveen, P., Lindahl, P., Hedstrand, H., Pekna, M., Hellstrom, M., Gebre-Medhin, S., Schalling, M., et al. (1996). PDGF-A signaling is a critical event in lung alveolar myofibroblast development and alveogenesis. Cell *85*, 863–873.

Casanovas, O., Hicklin, D.J., Bergers, G., and Hanahan, D. (2005). Drug resistance by evasion of antiangiogenic targeting of VEGF signaling in late-stage pancreatic islet tumors. Cancer Cell *8*, 299–309.

Cha, Y.R., and Weinstein, B.M. (2007). Visualization and experimental analysis of blood vessel formation using transgenic zebrafish. Birth Defects Res. C Embryo Today *81*, 286–296.

Chan, J., Bayliss, P.E., Wood, J.M., and Roberts, T.M. (2002). Dissection of angiogenic signaling in zebrafish using a chemical genetic approach. Cancer Cell *1*, 257–267.

Cohen, P.T. (2002). Protein phosphatase 1–targeted in many directions. J. Cell Sci. *115*, 241–256.

Cohen, P.T., Philp, A., and Vazquez-Martin, C. (2005). Protein phosphatase 4–from obscurity to vital functions. FEBS Lett. *579*, 3278–3286.

Cohen, P.T.W. (2004). Overview of protein serine/threonine phosphatases. In Topics in Current Genetics: Protein Phosphatases, J. Arino and D.R. Alexander, eds. (Berlin, Heidelberg: Springer-Verlag), pp. 1–20.

Cui, X., and Churchill, G.A. (2003). Statistical tests for differential expression in cDNA microarray experiments. Genome Biol. *4*, 210.

Eggert, U.S., Kiger, A.A., Richter, C., Perlman, Z.E., Perrimon, N., Mitchison, T.J., and Field, C.M. (2004). Parallel chemical genetic and genome-wide RNAi screens identify cytokinesis inhibitors and targets. PLoS Biol. *2*, e379.

Ekker, S.C. (2000). Morphants: a new systematic vertebrate functional genomics approach. Yeast *17*, 302–306.

Eldridge, R., and Casida, J.E. (1995). Cantharidin effects on protein phosphatases and the phosphorylation state of phosphoproteins in mice. Toxicol. Appl. Pharmacol. *130*, 95–100.

Ellis, L.M., and Hicklin, D.J. (2008). VEGF-targeted therapy: mechanisms of anti-tumour activity. Nat. Rev. Cancer *8*, 579–591.

Erdodi, F., Toth, B., Hirano, K., Hirano, M., Hartshorne, D.J., and Gergely, P. (1995). Endothall thioanhydride inhibits protein phosphatases-1 and -2A in vivo. Am. J. Physiol. *269*, C1176–C1184.

Eskens, F.A., and Verweij, J. (2006). The clinical toxicity profile of vascular endothelial growth factor (VEGF) and vascular endothelial growth factor receptor (VEGFR) targeting angiogenesis inhibitors; a review. Eur. J. Cancer *42*, 3127–3139.

Ferrara, N., Hillan, K.J., Gerber, H.P., and Novotny, W. (2004). Discovery and development of bevacizumab, an anti-VEGF antibody for treating cancer. Nat. Rev. Drug Discov. *3*, 391–400.

Fong, T.A., Shawver, L.K., Sun, L., Tang, C., App, H., Powell, T.J., Kim, Y.H., Schreck, R., Wang, X., Risau, W., et al. (1999). SU5416 is a potent and selective inhibitor of the vascular endothelial growth factor receptor (Flk-1/KDR) that inhibits tyrosine kinase catalysis, tumor vascularization, and growth of multiple tumor types. Cancer Res. *59*, 99–106.

Gaengel, K., Genové, G., Armulik, A., and Betsholtz, C. (2009). Endothelial-mural cell signaling in vascular development and angiogenesis. Arterioscler. Thromb. Vasc. Biol., in press. Published online January 22, 2009. 10.1161/ATVBAHA.107.161521.

Hartel, F.V., Rodewald, C.W., Aslam, M., Gunduz, D., Hafer, L., Neumann, J., Piper, H.M., and Noll, T. (2007). Extracellular ATP induces assembly and activation of the myosin light chain phosphatase complex in endothelial cells. Cardiovasc. Res. *74*, 487–496.

Knapp, J., Boknik, P., Luss, I., Huke, S., Linck, B., Luss, H., Muller, F.U., Muller, T., Nacke, P., Noll, T., et al. (1999). The protein phosphatase inhibitor cantharidin alters vascular endothelial cell permeability. J. Pharmacol. Exp. Ther. *289*, 1480–1486.

Knapp, J., Boknik, P., Linck, B., Luss, H., Muller, F.U., Petertonjes, L., Schmitz, W., and Neumann, J. (2000). Cantharidin enhances norepinephrine-induced vasoconstriction in an endothelium-dependent fashion. J. Pharmacol. Exp. Ther. *294*, 620–626.

Korff, T., and Augustin, H.G. (1998). Integration of endothelial cells in multicellular spheroids prevents apoptosis and induces differentiation. J. Cell Biol. *143*, 1341–1352.

Korff, T., and Augustin, H.G. (1999). Tensional forces in fibrillar extracellular matrices control directional capillary sprouting. J. Cell Sci. *112*, 3249–3258.

Kung, H.N., Chien, C.L., Chau, G.Y., Don, M.J., Lu, K.S., and Chau, Y.P. (2007). Involvement of NO/cGMP signaling in the apoptotic and anti-angiogenic effects of β-lapachone on endothelial cells in vitro. J. Cell. Physiol. *211*, 522–532.

Kwon, H.J. (2006). Discovery of new small molecules and targets towards angiogenesis via chemical genomics approach. Curr. Drug Targets *7*, 397–405.

Larson, J.D., Wadman, S.A., Chen, E., Kerley, L., Clark, K.J., Eide, M., Lippert, S., Nasevicius, A., Ekker, S.C., Hackett, P.B., et al. (2004). Expression of VE-cadherin in zebrafish embryos: a new tool to evaluate vascular development. Dev. Dyn. *231*, 204–213.

Li, L., Kozlowski, K., Wegner, B., Rashid, T., Yeung, T., Holmes, C., and Ballermann, B.J. (2007). Phosphorylation of TIMAP by glycogen synthase kinase-3β activates its associated protein phosphatase 1. J. Biol. Chem. *282*, 25960–25969.

Li, Y.M., Mackintosh, C., and Casida, J.E. (1993). Protein phosphatase 2A and its [3H]cantharidin/[3H]endothall thioanhydride binding site. Inhibitor specificity of cantharidin and ATP analogues. Biochem. Pharmacol. *46*, 1435–1443.

Martyn, U., and Schulte-Merker, S. (2004). Zebrafish neuropilins are differentially expressed and interact with vascular endothelial growth factor during embryonic vascular development. Dev. Dyn. *231*, 33–42.

Nasevicius, A., and Ekker, S.C. (2000). Effective targeted gene 'knockdown' in zebrafish. Nat. Genet. *26*, 216–220.

Oh, S.P., Seki, T., Goss, K.A., Imamura, T., Yi, Y., Donahoe, P.K., Li, L., Miyazono, K., ten Dijke, P., Kim, S., et al. (2000). Activin receptor-like kinase 1 modulates transforming growth factor-β 1 signaling in the regulation of angiogenesis. Proc. Natl. Acad. Sci. USA *97*, 2626–2631.

Ridgway, J., Zhang, G., Wu, Y., Stawicki, S., Liang, W.C., Chanthery, Y., Kowalski, J., Watts, R.J., Callahan, C., Kasman, I., et al. (2006). Inhibition of Dll4 signalling inhibits tumour growth by deregulating angiogenesis. Nature *444*, 1083–1087.

Romano, M., and Claria, J. (2003). Cyclooxygenase-2 and 5-lipoxygenase converging functions on cell proliferation and tumor angiogenesis: implications for cancer therapy. FASEB J. *17*, 1986–1995.

Ross-Macdonald, P. (2005). Forward in reverse: how reverse genetics complements chemical genetics. Pharmacogenomics *6*, 429–434.

Scheidl, S.J., Nilsson, S., Kalen, M., Hellstrom, M., Takemoto, M., Hakansson, J., and Lindahl, P. (2002). mRNA expression profiling of laser microbeam microdissected cells from slender embryonic structures. Am. J. Pathol. *160*, 801–813.

Shalaby, F., Rossant, J., Yamaguchi, T.P., Gertsenstein, M., Wu, X.F., Breitman, M.L., and Schuh, A.C. (1995). Failure of blood-island formation and vasculogenesis in Flk-1-deficient mice. Nature *376*, 62–66.

Shinoki, N., Sakon, M., Kambayashi, J., Ikeda, M., Oiki, E., Okuyama, M., Fujitani, K., Yano, Y., Kawasaki, T., and Monden, M. (1995). Involvement of protein phosphatase-1 in cytoskeletal organization of cultured endothelial cells. J. Cell. Biochem. *59*, 368–375.

Soares, M.B., Bonaldo, M.F., Jelene, P., Su, L., Lawton, L., and Efstratiadis, A. (1994). Construction and characterization of a normalized cDNA library. Proc. Natl. Acad. Sci. USA *91*, 9228–9232.

Tran, T.C., Sneed, B., Haider, J., Blavo, D., White, A., Aiyejorun, T., Baranowski, T.C., Rubinstein, A.L., Doan, T.N., Dingledine, R., et al. (2007). Automated, quantitative screening assay for antiangiogenic compounds using transgenic zebrafish. Cancer Res. *67*, 11386–11392.

Tsujii, M., Kawano, S., Tsuji, S., Sawaoka, H., Hori, M., and DuBois, R.N. (1998). Cyclooxygenase regulates angiogenesis induced by colon cancer cells. Cell *93*, 705–716.

Valdimarsdottir, G., Goumans, M.J., Itoh, F., Itoh, S., Heldin, C.H., and ten Dijke, P. (2006). Smad7 and protein phosphatase 1α are critical determinants in the duration of TGF-β/ALK1 signaling in endothelial cells. BMC Cell Biol. *7*, 16.

Visel, A., Thaller, C., and Eichele, G. (2004). GenePaint.org: an atlas of gene expression patterns in the mouse embryo. Nucleic Acids Res. *32*, D552–D556.

Wallgard, E., Larsson, E., He, L., Hellstrom, M., Armulik, A., Nisancioglu, M.H., Genove, G., Lindahl, P., and Betsholtz, C. (2008). Identification of a core set of 58 gene transcripts with broad and specific expression in the microvasculature. Arterioscler. Thromb. Vasc. Biol. *28*, 1469–1476.

Wang, E., Miller, L.D., Ohnmacht, G.A., Liu, E.T., and Marincola, F.M. (2000). High-fidelity mRNA amplification for gene profiling. Nat. Biotechnol. *18*, 457–459.

Wang, G.S. (1989). Medical uses of mylabris in ancient China and recent studies. J. Ethnopharmacol. *26*, 147–162.

Young, M.R., Kolesiak, K., and Meisinger, J. (2002). Protein phosphatase-2A regulates endothelial cell motility and both the phosphorylation and the stability of focal adhesion complexes. Int. J. Cancer *100*, 276–282.

Zhu, X., Wu, S., Dahut, W.L., and Parikh, C.R. (2007). Risks of proteinuria and hypertension with bevacizumab, an antibody against vascular endothelial growth factor: systematic review and meta-analysis. Am. J. Kidney Dis. *49*, 186–193.